

## Journal Pre-proofs

Discovery of a Series of Benzopyrimidodiazepinone TNK2 Inhibitors via Scaffold Morphing

Zhengnian Li, Chelsea E. Powell, Brian J. Groendyke, Thomas W. Gero, Frederic Feru, John Feutrill, Bailing Chen, Bin Li, Hilary Szabo, Nathanael S. Gray, David A. Scott

PII: S0960-894X(20)30567-9  
DOI: <https://doi.org/10.1016/j.bmcl.2020.127456>  
Reference: BMCL 127456

To appear in: *Bioorganic & Medicinal Chemistry Letters*

Received Date: 18 May 2020  
Revised Date: 23 July 2020  
Accepted Date: 24 July 2020

Please cite this article as: Li, Z., Powell, C.E., Groendyke, B.J., Gero, T.W., Feru, F., Feutrill, J., Chen, B., Li, B., Szabo, H., Gray, N.S., Scott, D.A., Discovery of a Series of Benzopyrimidodiazepinone TNK2 Inhibitors via Scaffold Morphing, *Bioorganic & Medicinal Chemistry Letters* (2020), doi: <https://doi.org/10.1016/j.bmcl.2020.127456>

This is a PDF file of an article that has undergone enhancements after acceptance, such as the addition of a cover page and metadata, and formatting for readability, but it is not yet the definitive version of record. This version will undergo additional copyediting, typesetting and review before it is published in its final form, but we are providing this version to give early visibility of the article. Please note that, during the production process, errors may be discovered which could affect the content, and all legal disclaimers that apply to the journal pertain.

© 2020 Published by Elsevier Ltd.





## Discovery of a Series of Benzopyrimidodiazepinone TNK2 Inhibitors via Scaffold Morphing

Zhengenian Li,<sup>a,b</sup> Chelsea E. Powell,<sup>a,b</sup> Brian J. Groendyke,<sup>a,b</sup> Thomas W. Gero,<sup>a,b</sup> Frederic Feru,<sup>a,b</sup> John Feutrill,<sup>d</sup> Bailing Chen,<sup>d</sup> Bin Li,<sup>d</sup> Hilary Szabo,<sup>c</sup> Nathanael S. Gray,<sup>a,b,\*</sup> and David A. Scott,<sup>a,b,\*</sup>

<sup>a</sup> Department of Cancer Biology, Dana-Farber Cancer Institute, Boston, MA 02115, USA.

<sup>b</sup> Department of Biological Chemistry & Molecular Pharmacology, Harvard Medical School, 360 Longwood Ave, Boston, MA 02115, USA.

<sup>c</sup> Vivid BioSciences, 50 Northern Ave, Boston, MA 02210, USA

<sup>d</sup> SYNthesis med chem, 425 Changyang Street, Suzhou Industry Park, Suzhou, Jiangsu, China.

### ARTICLE INFO

#### Article history:

Received

Revised

Accepted

Available online

#### Keywords:

TNK2

Kinase inhibitor

Benzopyrimidodiazepinone

Scaffold morphing

### ABSTRACT

The protein kinase TNK2 (ACK1) is an emerging drug target for a variety of indications, in particular for cancer where it plays a key role transmitting cell survival, growth and proliferative signals via modification of multiple downstream effectors by unique tyrosine phosphorylation events. Scaffold morphing based on our previous TNK2 inhibitor **XMD8-87** identified urea **17** from which we developed the potent and selective compound **32**. A co-crystal structure was obtained showing **32** interacting primarily with the main chain atoms of an alanine residue of the hinge region. Additional H-bonds exist between the urea NHs and the Thr205 and Asp270 residues.

2009 Elsevier Ltd. All rights reserved.

Tyrosine Kinase Nonreceptor 2 (TNK2) is a cytoplasmic kinase, and was originally identified based on its binding to the cell-cycle regulator, CDC42, also known as ACK1<sup>1,2</sup> (activated CDC42-associated kinase). TNK2 aberrant activation or mutation occurs in multiple types of cancers such as prostate, breast, schwannoma, pancreatic, ovarian, non-small cell lung cancer,<sup>3</sup> and leukemia.<sup>4</sup> TNK2 can interact with several oncogenic signaling pathways, including modulation of the AKT signaling pathway<sup>5</sup> and phosphorylation of androgen receptor, resulting in androgen-independent prostate cancer growth.<sup>6</sup> Additionally, TNK2 negatively regulates the tumor suppressor Wwox.<sup>7</sup> These findings suggest that inhibition of TNK2 might have therapeutic potential across various cancers.<sup>8</sup>

Several groups have reported small-molecule TNK2 inhibitors (Figure 1).<sup>9-13</sup> AIM-100 has been used as a tool compound to study TNK2 biology, though it was initially disclosed as a screening hit in a Lck inhibitor program.<sup>14</sup> Amgen reported a series of potent pyrazolopyrimidines and obtained an X-ray co-crystal structure with **2**, which showed the typical donor-acceptor H-bond interactions between the hinge and the anilinopyrimidine and an additional H-bond to the gatekeeper Thr205 residue from the dimethylaniline substituent.<sup>9</sup> Compound **3** was described by OSI as a relatively selective (KinomeScan S(10) = 0.08) TNK2 inhibitor with good oral PK.<sup>11</sup> Compound **4** was developed through the preparation of a library of compounds incorporating fragments of other TNK2 inhibitors, and has been used to explore the role of TNK2 in prostate and triple negative breast cancer.<sup>12</sup> We previously reported the benzopyrimidodiazepinone XMD8-

**87** as a potent and highly selective TNK2 inhibitor (Kinome Scan S(10) = 0.03), identified through kinase selectivity profiling.<sup>4,13</sup>

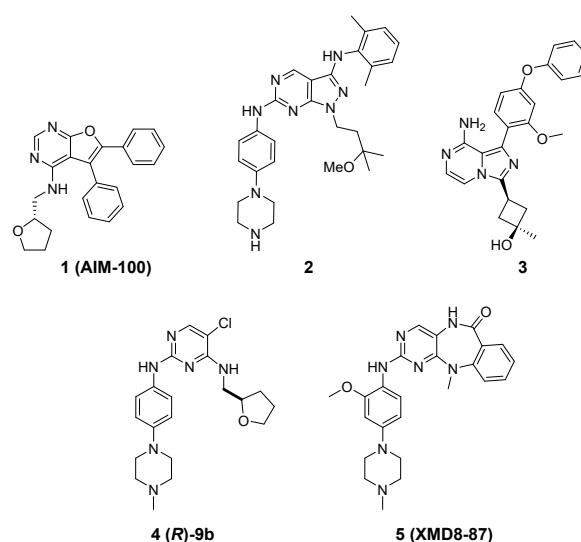


Figure 1. TNK2 inhibitors.

We also recently described our efforts to optimize the PK profile of the benzopyrimidodiazepinone series,<sup>15</sup> but observed consistently high in vivo clearance for compounds lacking a substituent on the amide nitrogen. This was in contrast to the amide N-methyl analogs reported as inhibitors of ERK5<sup>16</sup> and LRRK2,<sup>17,18</sup> which demonstrated good IV and oral PK profiles. We pursued a scaffold-morphing approach to try and develop

amide core of XMD8-87 was replaced with a urea scaffold.

An efficient three-step synthetic route was developed to prepare the urea compounds (17, 18, and 20-39). The synthesis is outlined in Scheme 1. First, a Suzuki coupling of 5-amino-2,4-dichloropyrimidine and a 2-aminophenylboronic acid pinacol ester gave diamine intermediate 8 in moderate yield. Treatment of the diamine with triphosgene at room temperature resulted in cyclization to the tricyclic urea intermediate 9. Anilines were installed on the pyrimidine of intermediate 9 via Pd coupling chemistry as the final step. Compound 19 was synthesized from methylamino phenylboronic acid pinacol ester 13, using similar procedures to those in Scheme 1. 13 was prepared in two steps from 2-aminophenylboronic acid pinacol ester 10 by alkylation with benzotriazole alcohol 11, and reduction of benzotriazole boronate ester 12 with sodium borohydride (Scheme 2).<sup>19</sup>

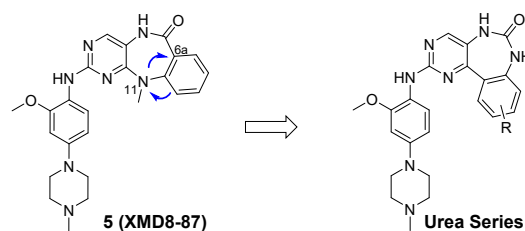
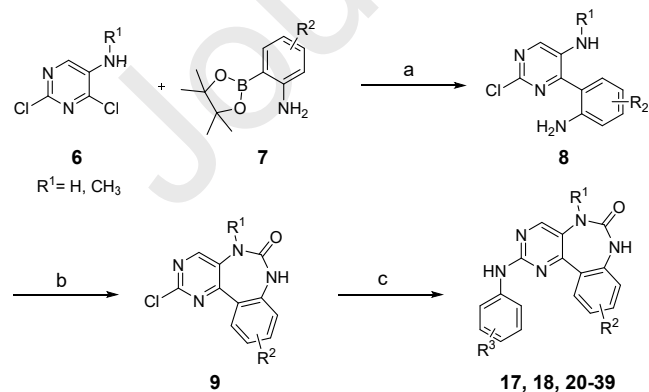


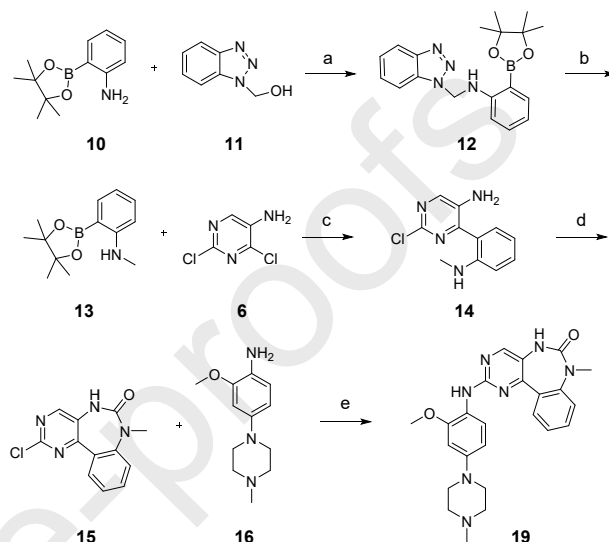
Figure 2. Scaffold morphing of amide to urea series.

To understand the structure-activity relationships (SAR) of the urea analogs, we employed a biochemical TNK2 assay (HTRF LanthaScreen Assay)<sup>20</sup> and a cell viability assay based on Ba/F3 cells expressing TNK2 D163E, (CellTiter-Glo Luminescent Cell Viability Assay).<sup>21</sup> We also conducted a cellular counter-screen assay in parental BaF3 cells, and observed at least 10 fold selectivity for the majority of compounds. Compound 17 (Table 1) had a TNK2 IC<sub>50</sub> of 738 nM, and an EC<sub>50</sub> of 0.48 μM in our Ba/F3 cellular assay, less potent than the amide XMD8-87 (IC<sub>50</sub> of 44 nM, cell EC<sub>50</sub> of 0.19 μM). We introduced a methyl group at each urea nitrogen (18, 19) but both compounds were significantly less active. This was consistent with our observations on the amide scaffold, in which a methyl group on the amide nitrogen of XMD8-87 led to reduced potency in both the enzyme and cell assays, with the NH adjacent to the pyrimidine ring assumed to make an H-bond interaction with the Thr205 gatekeeper of TNK2.



Scheme 1. Synthesis of benzopyrimidodiazepinones. Reagents and conditions: (a) Pd(dppf)Cl<sub>2</sub>, XPhos, 2.0 M Na<sub>2</sub>CO<sub>3</sub>/1,4-dioxane, 100°C, 4h, 49-74% yield; (b) Triphosgene, iPr<sub>2</sub>EtN, 1,4-dioxane, rt, 1h, 33-35% yield; (c) Aniline, XPhos, Pd<sub>2</sub>(dba)<sub>3</sub>, K<sub>2</sub>CO<sub>3</sub>, 1,4-dioxane, 100°C, 2h, 60-65% yield.

A methyl group was introduced at each position on the phenyl ring. 9-Methyl (21) and 10-methyl (22) demonstrated about 4-fold and 8-fold increase of potency in the biochemical assay (IC<sub>50</sub> = 224 nM) and (IC<sub>50</sub> = 91 nM) compared with 17. We also introduced fluorine at different positions of the phenyl ring, and further substituents at the C9 position, including methoxy (28) and cyclopropyl (27). Unlike the amide scaffold, in which even small substituents on the right-hand phenyl ring were not well-tolerated,<sup>15</sup> we found that several substituents on the phenyl ring of the urea scaffold led to increased TNK2 potency.



Scheme 2. Synthesis of 19. Reagents and conditions: (a) EtOH, rt, overnight, 70% yield; (b) NaBH<sub>4</sub>, THF, 75°C, 4 h, 69% yield; (c) Pd(dppf)Cl<sub>2</sub>, XPhos, 2.0 M Na<sub>2</sub>CO<sub>3</sub>/1,4-dioxane, 100°C, 4h, 35% yield; (d) Triphosgene, iPr<sub>2</sub>EtN, 1,4-dioxane, rt, 1h, 58% yield; (e) Pd<sub>2</sub>(dba)<sub>3</sub>, XPhos, K<sub>2</sub>CO<sub>3</sub>, 1,4-dioxane, 100°C, 2h, 60% yield.

Table 1. Phenyl ring SAR; compounds 17-28

Compound	R <sup>1</sup>	R <sup>2</sup>	R <sup>3</sup>	TNK2 IC <sub>50</sub> (nM) <sup>a</sup>	Cell TNK2 D163E (μM)	Cell Parental Ba/F3 (μM)
17	-	-	-	738	0.48	>10
18	Me	-	-	>10000*	5.87	nd
19	-	Me	-	4770	4.98	8.42
20	-	-	8-Me	942	0.21	2.77
21	-	-	9-Me	224	0.15	nd
22	-	-	10-Me	91	0.05	9.58
23	-	-	11-Me	1070	0.59	>10
24	-	-	8-F	248*	0.21	2.68
25	-	-	9-F	683	0.48	9.53
26	-	-	10-F	204	0.25	8.47
27	-	-	9-cyclopropyl	135	0.07	4.84
28	-	-	9-OMe	394	0.21	6.20

<sup>a</sup> Data was generated at BioDuro or ThermoFisher (\*). IC<sub>50</sub>s against TNK2 was obtained with LanthaScreen Binding activity assays and reported as the average of two replicates. nd = no data.

the 9-methyl substituted core (**21**), rather than the more potent 10-methyl substituted core (**22**) which showed a less selective kinase activity profile (data not shown here). Aniline SAR was generally consistent with what was previously observed for the amide series (Table 2). Compound **29**, lacking the 2-MeO group, was 2-fold more potent than **21** in the enzyme assay. Moving the methoxy group to the aniline 3-position (**30**) significantly improved TNK2 potency in both enzyme and cell assays. However, our previous data with the related benzopyrimidodiazepinone amide scaffold suggested that the 3-MeO aniline would result in reduced kinase selectivity.<sup>15</sup> We thought that 2-MeO substitution was most likely to give a good balance of potency and selectivity and focused on a set of anilines with this group with the potential to impact metabolism.<sup>22</sup>

**Table 2.** Enzyme and cell data for aniline SAR of 9-Me; compounds 21, 29-40

Compound	R	TNK2 IC50 (nM) <sup>a</sup>	Cell TNK2 D163E (μM)	Cell Parental Ba/F3 (μM)
<b>21</b>		224	0.15	nd
<b>29</b>		113	0.11	>10
<b>30</b>		13	0.02	5.62
<b>31</b>		164	0.34	6.56
<b>32</b>		102	0.29	9.93
<b>33</b>		3935	5.07	3.50
<b>34</b>		120	0.32	nd
<b>35</b>		405	0.58	8.53
<b>36</b>		3410	2.84	9.33
<b>37</b>		364	0.70	4.95
<b>38</b>		313	1.11	7.55
<b>39</b>		279	0.47	9.62

**40** 131 0.37 >10

<sup>a</sup> Data was generated at BioDuro. IC50s against TNK2 was obtained with LanthaScreen Binding activity assays and reported as the average of two replicates. nd = no data.

Piperazine derivatives **31** and **32** showed similar enzyme and cell potency to the *N*-methylpiperazine **21**. Fluorine was introduced to the phenyl ring to reduce its electron density and potential for oxidation. This resulted in reduced potency when the F was *ortho* to the aniline NH (**33**), but substitution at the meta position (**34**) was tolerated. We also installed *N*-methylpiperidines (**35**, **36**, and **37**) to avoid the possibility of 1,4-quinone diamine formation, but these compounds were consistently less potent than the piperazines. We also prepared a set of compounds with a bicyclic aniline<sup>15</sup> and of these, tetrahydroisoquinoline **40** was the most potent. Overall, there was a good correlation between the enzyme and TNK2 cell assays for the urea series.

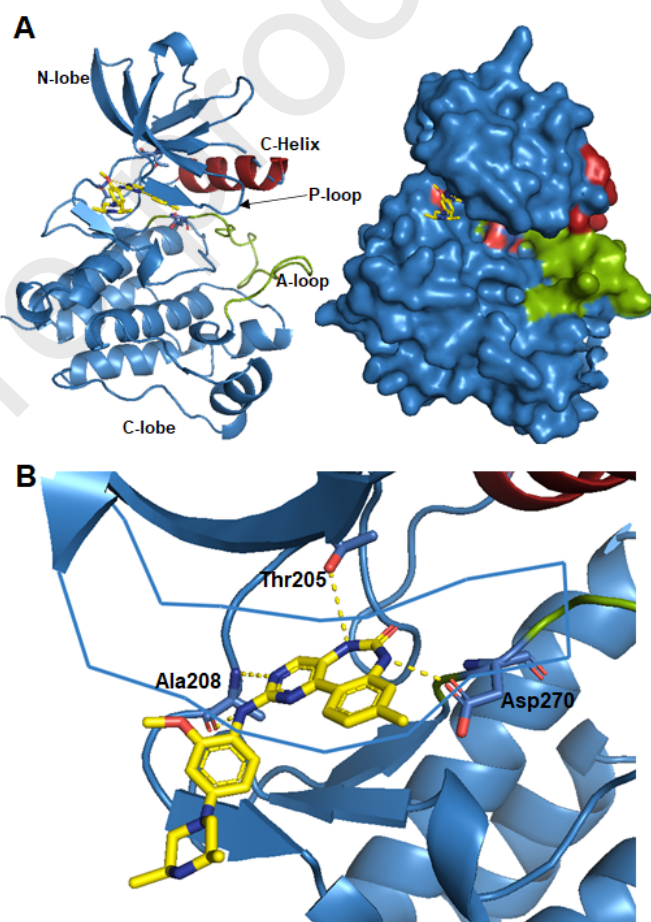


**Figure 3.** (A) X-ray co-crystal structure of TNK2 in complex with compound **32**, refined at 2.87 Å resolution (PDB: 6VPM). Compound **32** is shown in stick representation with yellow carbon atoms. (B) Hydrogen bonds are indicated by dotted lines. Main interacting residues are shown and labeled.

To confirm the binding mode of the urea series, we solved the co-crystal structure of compound **32** with TNK2 at a resolution of 2.87 Å with the ligand occupying the ATP site and neighboring regions (Figure 3A). As expected, the pyrimidine N and aniline NH interacted with the hinge, forming H-bonds with the amide NH and carbonyl of Ala208, respectively. The aniline substituent extended into the solvent channel. The urea NH adjacent to the pyrimidine interacted with the Thr205 gatekeeper residue, and this likely contributed to the overall kinase selectivity of the urea series, as we had suspected was the case for the previously

to the phenyl ring interacted with the Asp270 of the DFG motif at the beginning of the activation loop. Methylation at either of the urea nitrogens, to give compounds **18** and **19**, resulted in a significant loss of enzyme and cell potency. Compared to the amide series, the phenyl ring of the tricyclic urea scaffold is positioned in a more open region of the protein, allowing the introduction of substituents at several positions to further improve potency and selectivity.

We tested the kinase selectivity of **32** using KINOMEScan at a concentration of 1  $\mu$ M. The results show that **32** displays excellent kinase selectivity with an S (10) score of 0.01, calculated by dividing the number of kinases with ctrl%  $\leq$ 10% (n = 14) by the total number of kinases tested (n = 468). (See Supporting Table 1 and Figure 1 for the full data).

Metabolic stability of compounds **31** and **32** was assessed in mouse and human liver microsomes and mouse hepatocytes, and both compounds demonstrated good *in vitro* metabolic stability (Table 3). Compound **31** and **32** were further evaluated for their pharmacokinetic properties in male CD1 mice after intravenous (IV) and oral (PO) administration (Table 4). Hydroxyethylpiperazine **31** displayed a half-life ( $T_{1/2}$ ) of 0.6 h, a very high clearance (Cl) of 150 mL/min/kg, and a low oral bioavailability of 6%. Dimethylpiperazine **32** shows a limited improvement over compound **31**, with clearance (Cl) of 77 mL/min/kg and oral bioavailability of 9%. The disconnect between the *in vitro* and *in vivo* clearance was disappointing, and we speculated that despite the encouraging *in vitro* stability data, oxidation to the quinone diamine might still be involved. We therefore profiled an example with a bicyclic aniline (**40**) but its overall PK profile was similar to that of **32**.

**Table 4.** Mouse microsome and hepatocyte stability, and *in vivo* mouse PK<sup>a</sup> data (3mpk IV, 10mpk PO)

Compound ID	Mouse microsomes ( $T_{1/2}$ )	Mouse hepatocytes ( $T_{1/2}$ )	IV Cl (ml/min/kg)	IV $T_{1/2}$ (hr)	F %	Auc inf (PO) (ng*hr/ml)
<b>31</b>	57	>500	150	0.6	6	101
<b>32</b>	145	>500	77	1.8	9	200
<b>40</b>	-	-	94	1.8	18	405

<sup>a</sup> PK studies were conducted in male CD-1 mice, and all values are an average from three animals

## Acknowledgments

Ba/F3 cells expressing TNK2 D163E were generously provided by Jeffrey W. Tyner (Oregon Health and Science University, Portland, OR). *In vitro* and *in vivo* PK studies were conducted at BioDuro, Shanghai, under the supervision of Cindy Liang and Ying Zhou. Hyuk-Soo Seo helped upload the structural data to the PDB and Milka Kostic assisted with the preparation of the manuscript. We thank Vivid BioSciences for funding support.

## References and notes

- Prieto-Echague, V.; Miller, W. T. *J Signal Transduct* **2011**, *2011*, 742372.
- Mahajan, K.; Mahajan, N. P. *Cancer Letters* **2013**, *338* (2), 185.
- Mahajan, K.; Mahajan, N. P. *Oncogene* **2015**, *34* (32), 4162.
- Maxson, J. E.; Abel, M. L.; Wang, J. et al. *Cancer Res.* **2016**, *76*, 127.
- Mahajan, K.; Challa, S.; Coppola, D. et al. *Prostate* **2010**, *70* (12), 1274.
- Mahajan, N. P.; Liu, Y.; Majumder, S. et al. *Proc Natl Acad Sci U S A* **2007**, *104* (20), 8438.
- Mahajan, N. P.; Whang, Y. E.; Mohler, J. L. et al. *Cancer Res* **2005**, *65* (22), 10514.

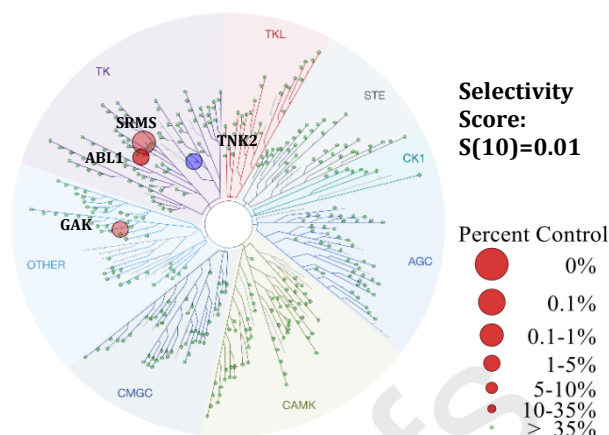


**Figure 4.** KINOMEScan results for compound **32**. Selectivity profile was determined for 468 kinases as percent DMSO control at 1  $\mu$ M inhibitor concentration (excluding mutant, lipid, atypical and pathogen). S (10) of compound **32** against kinases with ctrl%  $\leq$ 10% containing TNK2 highlighted as blue.

In summary, we have demonstrated a scaffold-morphing approach to discover a novel series of urea TNK2 inhibitors. The introduction of substituents on the phenyl ring improved the potency of the series relative to **17**. The expected binding mode of the series was confirmed by a co-crystal structure with **32**, and this compound was found to have a good overall kinase selectivity profile. However, as with our series of amide benzopyrimidodiazepinone TNK2 inhibitors, we were not able to identify an example with good PK, despite promising *in vitro* metabolic stability data.

- Fox, M.; Crafter, C.; Owen, D. *Biochem Soc Trans* **2019**, *47* (6), 1715.
- Kopecky, D. J.; Hao, X.; Chen, Y. et al. *Bioorg Med Chem Lett* **2008**, *18* (24), 6352.
- Jiao, X.; Kopecky, D. J.; Liu, J. et al. *Bioorg Med Chem Lett* **2012**, *22* (19), 6212.
- Jin, M.; Wang, J.; Kleinberg, A. et al. *Bioorg Med Chem Lett* **2013**, *23* (4), 979.
- Lawrence, H. R.; Mahajan, K.; Luo, Y. et al. *J Med Chem* **2015**, *58* (6), 2746.
- Miduturu, C. V.; Deng, X.; Kwiatkowski, N. et al. *Chem Biol* **2011**, *18* (7), 868.
- DiMauro, E. F.; Newcomb, J.; Nunes, J. J. et al. *Bioorg Med Chem Lett* **2007**, *17* (8), 2305.
- Groendyke, B. J.; Powell, C. E.; Feru, F. et al. *Bioorg Med Chem Lett* **2020**, *30* (4), 126948.
- Deng, X.; Yang, Q.; Kwiatkowski, N. et al. *ACS Med Chem Lett* **2011**, *2* (3), 195.
- Deng, X.; Dzamko, N.; Prescott, A. et al. *Nat Chem Biol* **2011**, *7* (4), 203.
- Deng, X.; Elkins, J. M.; Zhang, J. et al. *Eur J Med Chem* **2013**, *70*, 758.
- Ogiyama, T.; Yamaguchi, M.; Kurikawa, N. et al. *Bioorg Med Chem* **2017**, *25* (7), 2234.

using an HTK1 Luminescence assay. For compounds tested at both sites, there was an excellent correlation between the two assays, with the ThermoFisher assay typically showing slightly increased sensitivity (compounds up to 2-fold more potent).

21. We used a cell viability assay based on Ba/F3 cells expressing TNK2 D163E. Parental Ba/F3 cells were cultured with an additional 1 ng/mL recombinant mouse IL-3. Cells were plated at a volume of 50  $\mu$ L with a density of 105 cells/mL in white 384-well plates (Corning 3570). 100 nL of compound in DMSO from stock plates was added by pin transfer using a Janus Workstation

CellTiter-Glo Luminescent Cell Viability Assay (Promega) following the manufacturer's standards. IC50s were modeled from 3 biological replicates using GraphPad Prism 8 software.

22. Mesaros, E. F.; Thieu, T. V.; Wells, G. J. et al. *J Med Chem* **2012**, 55 (1), 115.

## Supplementary Material

Journal Pre-proofs